Influence of Temperature on Bond Wire Fatigue of Gate Loops in IGBT Modules under Sinusoidal Vibration Stress

Cao Zhan[1], Yaxin Zhang[1], Yizheng Tang[1], Francesco Iannuzzo[2], Lingyu Zhu[1], Shengchang Ji[1], Frede Blaabjerg[2]
[1] Xi'an Jiaotong University, China
[2] Aalborg University, Denmark

***Abstract*-- The vibration fatigue mechanism in IGBT modules is critical, while experimental data on this topic is still insufficient. In this paper, a vibration-temperature test platform for IGBT modules is developed, and the sinusoidal vibration tests are conducted in the y-axis direction. The location of the vibration-sensitive components is identified by observation after broken fault indicated by static characteristics. It is observed that the bond wires in gate loops are fragile components. Then, high-frequency impedance between the gate- and Kelvin-emitter terminals is proposed as condition monitoring indicator during the vibration test. The impedance can be reflected by the peak voltage of a sampling resistor, which has noticeable variation before the complete disconnection of the bond wire. The beginning of the variation is defined as the failure point, which is much earlier than seen in the static characteristics. Then the number of cycles to failure (NCF) is investigated at various temperatures. The NCF is found to decrease with temperature. Post-failure observations of all tested 48 modules under test are conducted.**

***Index Terms*-- IGBT module, bond wires, vibration test, NFC, gate loop, Kelvin-emitter**

I. INTRODUCTION

Historically, the temperature is by far the most critical factor that influences the lifetime of power semiconductor devices [1-3]. In that respect, thermo-mechanical long-term fatigue mechanisms on insulated-gate bipolar transistors (IGBTs) have been deeply investigated. Due to the difference in the coefficient of thermal expansion (CTE) of silicon and other materials, thermal stress is induced on the joints of the packaging structure, leading to bond wire fatigue, solder fatigue, aluminum metallization, etc [4-6]. Power cycling test (PCT) is a common approach to investigate the fatigue mechanisms and the corresponding characteristic drift of the power modules [7-10]. The existing standards define the test specifications and end-of-life (EOL) criteria for IGBT modules [11-13].

With the rapid development of electric vehicles (EVs) and hybrid electric vehicles (HEVs), the reliability of IGBT module against vibration has drawn larger and larger attention in the last ten years. Power inverters have been placed closer and closer to the electrical motor to match both the power density- and the efficiency demand. These more and more compact structures inevitably carry along a significant amount of vibrations transmitted from the motor to the power inverter. Therefore, a deeper insight into the vibration fatigue of electrical components is needed to be understood.

Notably, the reliability of solder interconnection on the printed circuit board (PCB) against mechanical load (random vibration, vibration shock and sweep sinusoidal vibration) have been massively investigated in last decade [14-16]. The remining useful life [17], condition monitoring method [18], and finite-element modelling method [19] of solder joint have been investigated in-depth. Furthermore, the combined effect of power- and vibration load on the solder joints have been studied [20].

Different from the solder joints on PCB, the reliability assessment of IGBT modules against vibration is not sufficient. K. Sasaki et al. [21] conducted a numerical simulation to evaluate the fatigue life of aluminum wires under a random vibration test in terms of the temperature-dependent viscoelastic behavior of silicone gel. As a critical outcome, it was found that the frequency response, i.e., amplitude vs. acceleration, decreased above 50 Hz. More recently, mechanical stress prediction model considering more detailed packaging structure of IGBT modules were proposed. Jiajia Guan et al. [22] numerically investigated the influence of baseplate properties, i.e. footprint, thickness and material, on the corresponding solder stress under random vibration. Yanzhong Tian et al. [23] simulated the mechanical stress distribution on the root part of the bond wire under both harmonic- and random vibration without taking the viscoelastic effect of silicone gel into account. In addition to the mechanical stress distribution of the packaging components inside IGBT modules, H. Wang proposed a modal analysis of IGBT modules based on numerical simulation [24]. P. Rajaguru et al. [25] studied the vibration response in IGBT modules in a simplified structure without molding compound and bond wires. The same paper evaluated the combined effect of both vibrational and thermo-mechanical stimulus using a linear damage superposition method.

However, the experimental investigations are somewhat limited. The investigations of bond wire interconnection under vibration-temperature test environment have though been conducted to exhibit the fatigue mechanism and the influence of wire loop height and length [26]. The viscoelastic effect of silicone gel on the vibration fatigue of bond wires in IGBT modules was

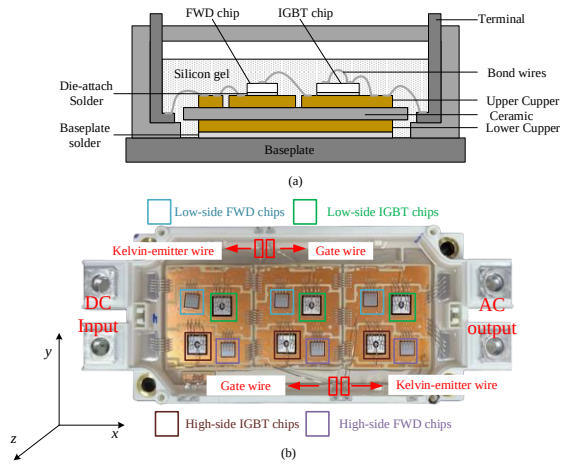

Fig. 1. DUT: (a) Cross-section diagram (b) physical appearance

not considered either. A remaining-useful-life model based on the experimental mixed-vibration-temperature stress was proposed in [27]. The vibration test was conducted under three different temperatures, but the influence of temperature on vibration fatigue characteristics was not specifically analyzed. The combined effect of vibrational shock and thermomechanical fatigue were simultaneously investigated in [28]. The influence of temperature on the vibration fatigue was not included either. In conclusion, the research done so far lacks an investigation of the influence of temperature on vibration fatigue mechanism.

This paper develops a vibration-temperature test platform for IGBT modules to investigate this specific issue and determine the number of cycles to failure (NCF) at various temperatures under the sinusoidal vibration in y-axis direction. The paper is organized as follows: Section II introduces the structure of the considered IGBT modules as well as the developed and used vibration-temperature test platform. Section III shows the obtained results under the vibration test and the related post-failure analyses. The last section draws the conclusions of this work.

II. Device under Test and Vibration-Temperature Test Platform

A. Device under Test

A traditional half-bridge commercial IGBT module (FF150R12ME3G) rated 1200V and 150 A is used as a device under test (DUT). Fig. 1(a) shows its cross-section principle, whereas its physical structure is shown in Fig. 1(b). IGBT chips and free-wheeling diode (FWD) chips are attached to a DBC (Direct Bond Copper - it consists of upper copper, ceramic and lower copper) by means of a solder and the DBC is attached to a baseplate by means of another solder layer. Aluminum wires are used for the top-side electrical connection. The module comprises three identical paralleled half-bridge sections, each including a high-side IGBT, a low-side IGBT, a high-side FWD, and a low-side FWD. Bond wires are placed on the active areas of IGBT and FWD chips and on the power terminals, i.e.,

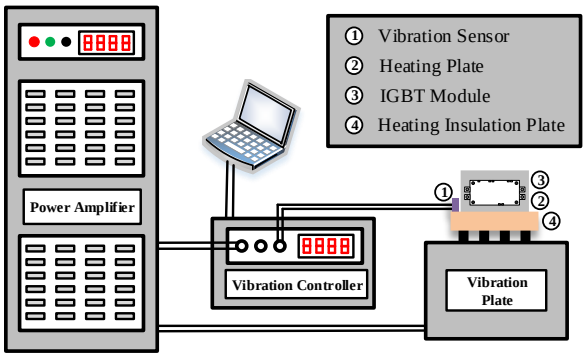

Fig. 2. Diagram of the vibration-temperature test platform

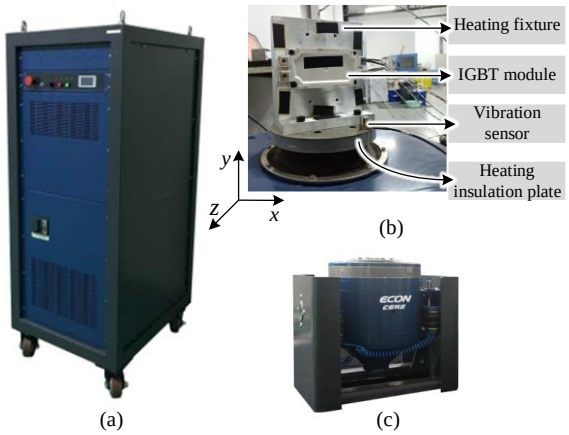

Fig. 3. Physical appearance of the test platform: (a) Power amplifier, (b) Fixture detail, and (c) Vibration plate.

DC-Input and AC-Output, for the power connections, while twelve (2 wires x 2 sides x 3 sections) gate and Kelvin-emitter wires connect IGBT gate pads to the related control terminals.

B. Vibration - Temperature Test Platform

A schematic of the vibration-temperature test platform is shown in Fig. 2, which consists of a power amplifier (VSA-H402A), a computer-based vibration controller (ECON VT-9008), and a vibration plate (EDS-300). Fig. 3(a), 3(b), and 3(c) show the power amplifier, details of the test fixture, and the vibration plate, respectively. The control loop starts from the vibration sensor, which monitors the DUT acceleration. Based on it, the vibration controller generates a control signal for the power amplifier to excite the vibration generator.

The DUT is mounted on a heating fixture. The working temperature of the heating fixture ranges from 30 °C to 300 °C. Notably, since the maximum working temperature of the vibration generator is below 40 °C, a heating insulation plate made of mica is placed between the heating fixture and the vibration plate. Three kinds of vibration profiles are offered by the platform, which are sinusoidal, random, and shock vibration. We chose the first profile for the study. The maximum acceleration is limited by the vibration thrust and the mass of the tested

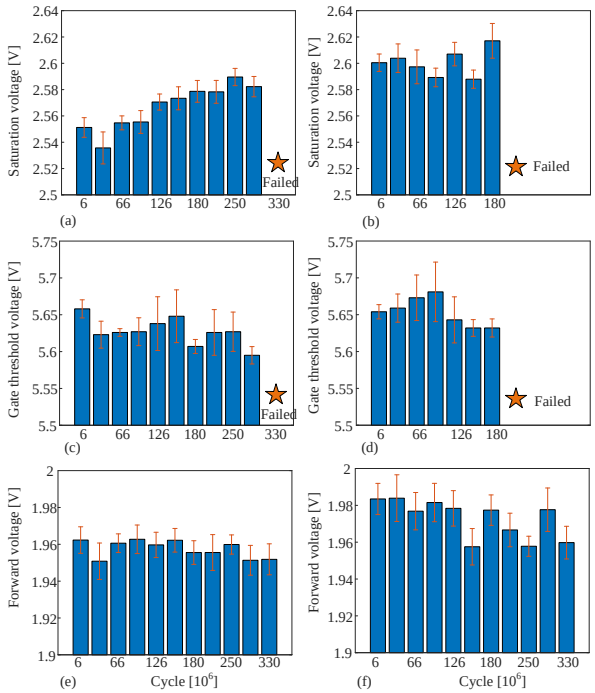

Fig. 4 Off-line static characterization during the vibration test. a)-f) Left: high-side IGBT; right: low-side IGBT. Top down: IGBT saturation voltage, IGBT threshold voltage, and FWD forward voltage.

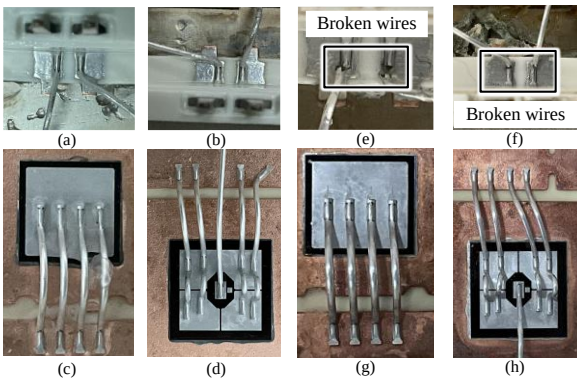

Fig. 5. Observed results after the static test: a)-d): healthy sample; e)-h): broken sample. from a) to d) and from e) to -h): gate- and kelvin-emitter wires of high-side IGBT, gate- and kelvin-emitter wires of low-side IGBT, wires on FWD active area, and wires on IGBT active area, respectively.

components. The vibration direction of the plate is the y-axis shown in Fig. 3(b).

III. Vibration Test Results

The vibration-sensitive location was identified after the static test. Notably, the static characterization process was performed offline, i.e., stopping the vibration test and measure the corresponding value of the static electrical parameters under the same condition. When the static characterization failed, the condition of the DUT was considered a completely broken fault. Then, the silicone gel of the DUT was removed to observe the condition of bond wires and identify the vibration-sensitive location. After that, online monitoring approach for the defect components was proposed to characterize the degradation process and count the NCF. Moreover, the influence of the temperature on the NCF was investigated.

A. Identification of the Vibration-Sensitive Location

One DUT was tested under 440 Hz, 25 g, and 125 °C. The selected frequency and acceleration were limited by the power rating of the vibration plate. The saturation voltage and the threshold voltage as well as the FWD forward voltage were measured off-line, i.e., stopping the vibration test and performing a static characterization. Multiple repetitions were conducted to reduce the uncertainties. Fig. 4(a) and (b) show the change in the saturation voltage of the high-side IGBT and the low-side IGBT during the test, while Fig. 4(c) and (d) show the change in the threshold voltage of the high-side IGBT and the low-side IGBT, respectively. The above results reveal that the high-side IGBT fails after 290 million cycles, while the low-side IGBT fails after 180 million cycles. The threshold voltage measurement also indicates a failure after 290 million cycles for the high-side IGBT, and after 180 million cycles for the low-side IGBT. Therefore, it can be concluded that either the gate wire or the Kelvin-emitter wire in the gate loop eventually fail. Fig. 4(e) and (f) show the measurement results of the forward voltage of high-side and low-side FWDs, respectively. The condition of FWD bond wires is healthy.

After the vibration test, the failed sample and a brand new IGBT module have been disassembled for a post-failure analysis, where the results have been shown in Fig. 5. Both the gate- and Kelvin-emitter bond wires of both high- and low- side IGBT broke, while the bond wires in the power loop remained healthy. The post-failure analysis could draw the conclusion that a disconnection of the gate and Kelvin-emitter wires are the key failure mechanism.

B. Condition Monitoring Approach

The high-frequency impedance between the gate- and Kelvin-emitter terminals was proposed as the online condition monitoring indicator during the vibration test. The impedance was reflected by the peak voltage of an in-series sample resistor. Thereby, an online monitoring system for the condition of the bond wires in the gate loop was implemented, as shown in Fig. 6. Two identical monitoring circuits, one for the high side and the other for the low side, comprised a signal generator, a 1-kOhm resistor, and a data acquisition system. Considering the gate capacitance, a 10 kHz-, 5V peak to peak sinusoidal voltage was supplied between the gate- and Kelvin-emitter terminals of both high- and low-side IGBT. When the condition of the gate- or Kelvin-emitter bond wires is abnormal, the voltage across the resistor will change. The voltage across the resistor was the input to the data acquisition system with a coaxial cable.

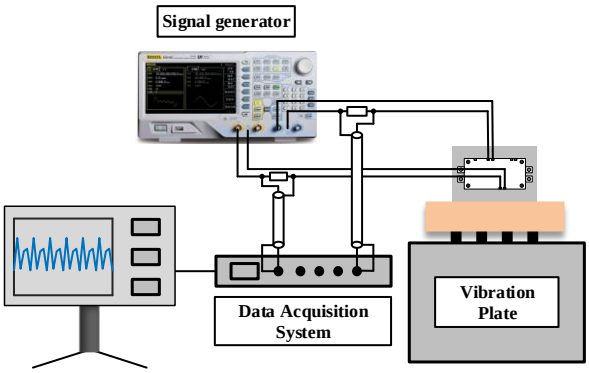

Fig. 6. Details of the condition monitoring approach

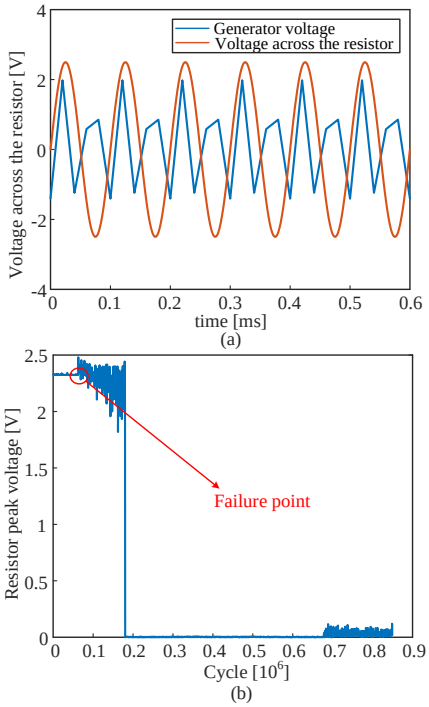

Fig. 7. On-line monitoring signals: (a) typical generator voltage and voltage across the resistor (b) resistor peak voltage vs. the number of cycles

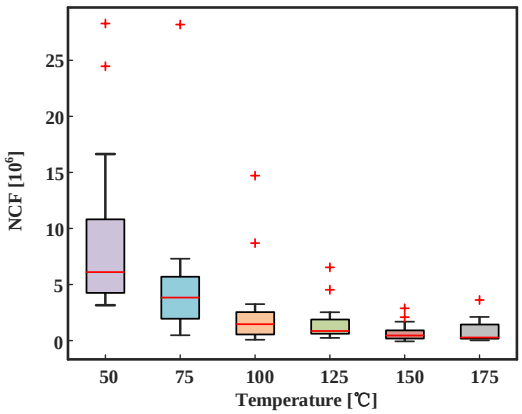

Fig. 8. Boxplot of the NCF under various temperature (440Hz and 25g)

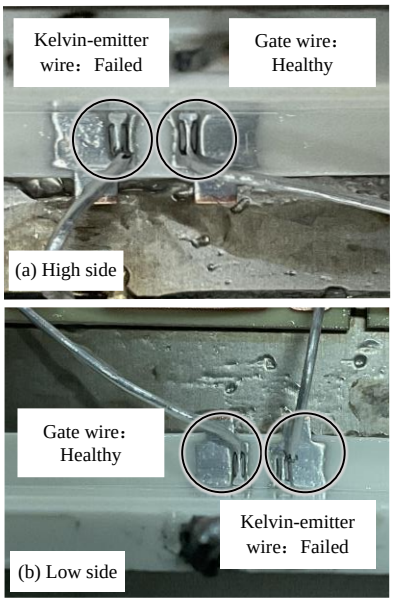

Fig. 9. Post-failure observation results after on-line NCF monitoring: (a) high side (b) low side

Both the generator voltage and the voltage across the resistor are shown in Fig. 7(a). Due to the limit of the maximum sampling frequency (50 kHz) of the data acquisition system, the waveform of the voltage across the resistor is not very smooth. Still, it does not affect the monitoring process. The resistor peak voltage vs. the number of cycles is shown in Fig. 7(b), revealing that the condition of the gate- and Kelvin-emitter wires are healthy at the primary stage. After that, the abnormality of the bond wire is detected, which is reflected in the variation of the resistor peak voltage. The silicone gel is encapsulated inside the module to maintain the position of the bond wire. When identifying the vibration-sensitive location, the static characterization was performed at the pause of the vibration test during the parameter measurement process. The encapsulated silicone gel ensures the connection of the abnormal bond wire under non-vibration status, resulting in an incorrect condition judgment of the corresponding bond wires. On the contrary, during the online monitoring process, the two parts of the abnormal wire have relative displacement under vibration excitation, leading to the variation of the resistor peak voltage. The beginning of a noticeable variation is defined as the failure point (seen in Fig. 7), which is much earlier than the reflection in static characteristics. Thus, the online monitoring of the abnormal condition of the bond wires in the gate loop should be implemented during the vibration test. The proposed indicator can effectively reflect the condition of the bond wire, and count the number of cycles to failure (NCF) at various temperatures under sinusoidal vibration.

C. Influence of Temperature on NCF

The corresponding number of cycles counted according to the failure point is regarded as the NCF. The obtained NCFs are listed in Table I for eight samples at six different temperatures. A total of 48 samples named #1-#48 were tested in this paper. A boxplot of the results of Table I is

TABLE I
NCF AT VARIOUS TEMPERATURE

Number	Position	50 ℃	75 ℃	100 ℃	125 ℃	150 ℃	175 ℃
#1-#6	High side	24469720	5615720	518760	1062160	1683000	164560
	Low side	5748160	2559920	71280	885720	88440	36080
#7-#12	High side	11737440	28188160	3248960	766040	403480	103400
	Low side	6996880	5777640	1829960	4529360	186120	51920
#13-#18	High side	8559760	2618440	8695280	624800	2086040	79200
	Low side	3153480	3020160	1213960	6534440	877360	306680
#19-#24	High side	28280560	949960	1705880	593560	947760	1664960
	Low side	3969680	708400	2567840	434280	99000	2111120
#25-#30	High side	6463600	4657840	600600	242880	218240	1013760
	Low side	16635960	478280	683320	820160	179960	1611720
#31-#36	High side	4167240	7303560	14710520	2530880	534160	56320
	Low side	3183400	5280880	2517240	2265560	443080	1251800
#37-#42	High side	4465560	6849480	2030600	286000	2879360	242880
	Low side	4682480	1961520	374000	952600	463760	3620320
#43-#48	High side	10020120	4655640	1041040	666160	24640	363000
	Low side	4746280	1939520	324280	1493800	593560	106040

@ 25g and 440 Hz vibration

shown in Fig. 8, revealing that temperature has a significant influence on the NCF. The average NCF decreases with the temperature.

D. Post-failure Analysis

After the online monitoring of each DUT, post-failure analysis was performed. Unlike the complete broken fault seen after the off-line static characterization, only terminal ends of Kelvin-emitter wires of both high- and low-side IGBT gate loops failed in these tests, and they are shown in Fig. 9.

This phenomenon has been observed in all failed 48 samples. The vibration test was stopped automatically depending on the falling edge of the resistor peak voltage in Fig. 7(b), which avoids further degradation and even more severe failures. Most interestingly, the terminal ends in the Kelvin-emitter wires for all cases with the condition monitoring approach during the vibration test.

IV. CONCLUSIONS

The bond wire fatigue of the gate loops in IGBT modules under sinusoidal vibration tests in the y-axial direction is investigated in this paper. Three important conclusions are drawn:

(1) The proposed high-frequency impedance reflected by the peak voltage of an in-series sample resistor during the vibration test can effectively monitor the condition of the bond wires in the gate loop. The resistor peak voltage has noticeable variation before the disconnection of the bond wire.

(2) The beginning of the apparent variation is defined as the end of life, and the obtained NCF decreases with the temperature.

An in-depth investigation and understanding of the vibration fatigue mechanism and characteristics at various temperature will be the next work to be done by a mechanical stress prediction model of bond wires inside silicone gel taking into the viscoelastic effect into account.

REFERENCES

[1] W. Lai, M. Chen, L. Ran, et al., "Low ΔTj Stress Cycle Effect in IGBT Power Module Die-Attach Lifetime Modeling," *IEEE Transactions on Power Electronics*, vol. 31, no. 9, pp. 6575-6585, Sept. 2016.

[2] U.M. Choi, F. Blaabjerg and S. Jørgensen, "Study on Effect of Junction Temperature Swing Duration on Lifetime of Transfer Molded Power IGBT Modules," *IEEE Transactions on Power Electronics*, vol. 32, no. 8, pp. 6434-6443, Aug. 2017.

[3] M. Hernes, S. D'Arco, A. Antonopoulos, et al., "Failure analysis and lifetime assessment of IGBT power modules at low temperature stress cycles," *IET Power Electronics*, vol. 14, no. 7, pp. 1271-1283, Apr. 2021.

[4] Y. Huang, Y. Jia, Y. Luo, et al., "Lifting-Off of Al Bonding Wires in IGBT Modules Under Power Cycling: Failure Mechanism and Lifetime Model," *IEEE Journal of Emerging and Selected Topics in Power Electronics*, vol. 8, no. 3, pp. 3162-3173, Sept. 2020.

[5] Y. Huang, H. Deng, Y. Luo, et al., "Fatigue Mechanism of Die-Attach Joints in IGBTs Under Low-Amplitude Temperature Swings Based on 3D Electro-Thermal-Mechanical FE Simulations," *IEEE Transactions on Industrial Electronics*, vol. 68, no. 4, pp. 3033-3043, April 2021.

[6] J. Zhao, T. AN, C. Fang, et al., "A Study on the Effect of Microstructure Evolution of the Aluminum Metallization Layer on Its Electrical Performance During Power Cycling," *IEEE Transactions on Power Electronics*, vol. 34, no. 11, pp. 11036-11045, Nov. 2019.

[7] U.M. Choi, F. Blaabjerg and S. Jørgensen, "Power Cycling Test Methods for Reliability Assessment of Power Device Modules in Respect to Temperature Stress," *IEEE Transactions on Power Electronics*, vol. 33, no. 3, pp. 2531-2551, March 2018.

[8] U.M. Choi, K. Ma and F. Blaabjerg, "Validation of Lifetime Prediction of IGBT Modules Based on Linear Damage Accumulation by Means of Superimposed Power Cycling Tests," *IEEE Transactions on Industrial Electronics*, vol. 65, no. 4, pp. 3520-3529, April 2018.

[9] N. Dornic, Z. Khatir, S. Tran, et al., "Stress-Based Model for Lifetime Estimation of Bond Wire Contacts Using Power Cycling Tests and Finite-Element Modeling," *IEEE Journal of Emerging and Selected Topics in Power Electronics*, vol. 7, no. 3, pp. 1659-1667, Sept. 2019.

[10] S. -H. Tran, Z. Khati, R. Lallemand, et al., "Constant ΔTj Power Cycling Strategy in DC Mode for Top-Metal and Bond-Wire Contacts Degradation Investigations," *IEEE Transactions on Power Electronics*, vol. 34, no. 3, pp. 2171-2180, March 2019.

[11] Power cycling ESD22-A122A, JEDEC solid date technology association, June 2016.

[12] IEC 60749-34 Semiconductor devices-Mechanical and climatic test methods-Part 34: power cycling, international standard, Geneva, Switzerland, 2010.

[13] ECPE Guideline AQG 324: Qualification of power module for use in power electronics converter units in motor vehicles. Nuremberg, Germany, May 2019.

[14] B. Gadalla, E. Schaltz and F. Blaabjerg, "A survey on the reliability of power electronics in electro-mobility applications," *2015 Intl Aegean Conference on Electrical Machines & Power Electronics (ACEMP), 2015 Intl Conference on Optimization of Electrical & Electronic Equipment (OPTIM) & 2015 Intl Symposium on Advanced Electromechanical Motion Systems (ELECTROMOTION)*, Side, Turkey, 2015, pp. 304-310.

[15] P. Lall, S. Gupte, P. Choudhary, et al., "Solder Joint Reliability in Electronics Under Shock and Vibration Using Explicit Finite-Element Submodeling," *IEEE Transactions on Electronics Packaging Manufacturing*, vol. 30, no. 1, pp. 74-83, Jan. 2007.

[16] M. Kavitha, Z. H. Mahmoud, K. H. Kishore, et al., "Application of Steinberg Model for Vibration Lifetime Evaluation of Sn-Ag-Cu-Based Solder Joints in Power Semiconductors," *IEEE Transactions on Components, Packaging and Manufacturing Technology*, vol. 11, no. 3, pp. 444-450, March 2021.

[17] N. Muhammad, Z. Fang, M. Shoaib, "Remaining useful life (RUL) estimation of electronic solder joints in rugged environment under random vibration," *Microelectronics Reliability*, vol. 107, 113614, Apr 2020.

[18] P. Lall, P. Gupta and A. Angral, "Anomaly Detection and Classification for PHM of Electronics Subjected to Shock and Vibration," *IEEE Transactions on Components, Packaging and Manufacturing Technology*, vol. 2, no. 11, pp. 1902-1918, Nov. 2012.

[19] P. Lall, S. Gupte, P. Choudhary, et al., "Solder Joint Reliability in Electronics Under Shock and Vibration Using Explicit Finite-Element Submodeling," *IEEE Transactions on Electronics Packaging Manufacturing*, vol. 30, no. 1, pp. 74-83, Jan. 2007.

[20] J. S. Karppinen, J. Li and M. Paulasto-Krockel, "The Effects of Concurrent Power and Vibration Loads on the Reliability of Board-Level Interconnections in Power Electronic Assemblies," *IEEE Transactions on Device and Materials Reliability*, vol. 13, no. 1, pp. 167-176, March 2013.

[21] K. Sasaki, N. Ohno, "Fatigue life evaluation of aluminum bonding wire in silicone gel under random vibration testing," *Microelectronics Reliability*, vol. 53, no. 9, pp. 1766-1770, July 2013.

[22] J. Guan, C. Zhang, C. Chen, et al., "Analysis of the Influence of Vibration and Thermal Vibration Coupling on the Power Module," *2021 IEEE Workshop on Wide Bandgap Power Devices and Applications in Asia (WiPDA Asia)*, Wuhan, China, 2021, pp. 23-26.

[23] Y. Tian, T. An, F. Qin, et al., "Stress analysis of automotive IGBT module under vibration load," *2022 23rd International Conference on Electronic Packaging Technology (ICEPT)*, Dalian, China, 2022, pp. 1-4.

[24] H. Wang, D. Liu, Y. Fan, et al, "Modal analysis of IGBT power devices based on ANSYS," *2019 20th International Conference on Electronic Packaging Technology (ICEPT)*, 2019, pp. 1-4.

[25] P. Rajaguru, H. Lu, C. Bailey, et al, "Modelling and analysis of vibration on power electronic module structure and application of model order reduction," *Microelectronics Reliability*, vol. 110, pp. 113697, May 2020.

[26] M. Mirgkizoudi, C. Liu, Conway P. Conway, et al., "Combined Temperature and Vibration Testing for Wire Bond Interconnections in Harsh Environment Electronics," *Journal of Microelectronics and Electronic Packaging*, vol. 10, no. 2, pp. 80-88, Jan. 2012.

[27] Wu H, Ye C, Zhang Y, et al., "Remaining Useful Life Prediction of an IGBT Module in Electric Vehicles Statistical Analysis," *Symmetry*, vol. 12, no. 8, pp. 1-13, Dec. 2020.

[28] V. Samavatian, M. Fotuhi-Firuzabad, P. Dehghanian, et al, "Reliability Modeling of Multistate Degraded Power Electronic Converters with Simultaneous Exposure to Dependent Competing Failure Processes," *IEEE Access*, vol. 9, pp. 67096-67108, 2021.